JOM
https://doi.org/10.1007/s11837-022-05664-8

Advances in Sintering of Titanium Aluminide: A Review

M.R. MPHAHLELE ,[1,2,4] P.A. OLUBAMBI,[2] and E.A. OLEVSKY[3]

1.—Department of Mechanical Engineering, Durban University of Technology, Durban 4001, South Africa. 2.—Centre for Nanomechanics and Tribocorrosion, School of Mining, Metallurgy and Chemical Engineering, University of Johannesburg, Johannesburg, South Africa. 3.—Powder Technology Laboratory, College of Engineering, San Diego State University, San Diego, CA, USA. 4.—e-mail: ramimphahlele@gmail.com

Titanium aluminides (TiAl) are prominent advanced materials for aerospace and automobile industries owing to their great engineering properties conferred by ordered structures and partial covalent bonding. Of all the TiAl phases, Ti_3Al and TiAl are considered to have great engineering significance and, thus, are extensively examined and developed for elevated temperature conditions. Nevertheless, one of the impediments to the wider application of TiAl and Ti_3Al alloys is the deficit in the malleability at room temperature, creating difficulties during fabrication as it is sensitive to microcracks and highly susceptible to superficial defects. Sintering technologies such as cold pressing, cold isostatic pressing, hot pressing, hot isostatic pressing, combustion synthesis, and microwave sintering for producing advanced TiAl are presented. However, these processes have restrictions on the control of the microstructural properties and phase evolution, which inevitably affect the quality of the TiAl products. The novel spark plasma sintering (SPS) offers opportunities to circumvent challenges existing in the production of TiAl. An innovative hybrid spark plasma sintering technology with great potential for large-scale fabrication of operational materials with improved microstructural characteristics yielding exceptional product value and enhanced design autonomy is also presented as a robust alternative for sintering TiAl alloys.

INTRODUCTION

The rise in the demand for materials with improved properties over a wide range of modern industrial environments has encouraged scientists to develop advanced engineering materials that offer excellent engineering properties. One such material is titanium aluminide (TiAl), which offers progressive solutions that include breakthroughs in the performance of the advanced materials in high temperatures, corrosive and excessive wear environments, and significant component weight reduction due to their low densities.[1] Given these arrays of benefits of TiAl, they are fast finding applications in automobile and aerospace industries, particularly in turbine engines.[2,3] According to Clemens and Kestler,[1] TiAl-based alloys offer tremendous advantages in a jet turbine engine, such as excellent stiffness and high temperature creep resistance. The alloy is also attractive for automotive engine applications in creating high-performance and fuel-efficient exhaust engine valves.

Despite the tremendous array of benefits offered by TiAl, its wide use is limited because of a deficit in the room temperature ductility of the alloy. Furthermore, over the past years, intense research in the TiAl reveals that the major types of alloy, alpha 2 (α_2)—TiAl and gamma (γ)—TiAl, by themselves have insignificant engineering relevance.[4] The significance of TiAl to engineering applications becomes prevalent when the two phases co-exist, especially in the region where aluminum content is between 40% and 48%. Therefore, recent and growing research development and innovative efforts are being directed toward ($\alpha_2 + \gamma$) TiAl alloys and composites.[5,6] Much consideration is also geared toward

(Received August 9, 2022; accepted December 16, 2022)

Published online: 24 January 2023

finding optimal manufacturing processes to ensure maximum performance and reduction in production costs of these materials.

Until now, PM sintering techniques are suitable candidates to produce TiAl alloys. The sintering techniques have proved to be superior to various ingot metallurgical manufacturing methods such as casting, rolling, and forging,[7] as materials produced via these conventional methods often show microstructure segregation.[8–10] Generally, sintering avoids some of these melting and casting problems due to increased processing rate and provides the opportunity for producing finer and homogeneous microstructure.[11] Some of the PM methods have also been identified as an environmentally friendly processing methods to produce Al/Ti-based materials cost-effectively,[12–15] particularly when considering the increase in the cost of raw materials.

Methods such as combustion synthesis and microwave sintering have been explored and some success was obtained in forming TiAl with required mechanical properties.[16,17] Other popular techniques such as cold pressing and sintering[18–20] and hot pressing[20] are reported in the literature. The limitations of these processing methods vary and range from the thermal gradient, grain growth, porosity, and inhomogeneity of materials. Furthermore, due to the intricate thermal and thermomechanical treatments, most of these PM pressing methods require several costly steps such as heat treatments processes, e.g., annealing[21] and tempering,[22] to accomplish a satisfactory microstructure.[23] However, recently the SPS was developed as an alternative technique and has received remarkable interest as a means for consolidating the innovative TiAl materials.[24] This vast interest is primarily due to the favorable features of SPS such as fast heating and cooling rates during sintering, making it feasible to easily control the formation of phases and grain size,[24–26] tailoring the engineering properties for numerous applications.

This paper reviews some conventional sintering techniques used in the manufacturing of titanium aluminide alloys and presents the novel spark plasma sintering technology as an attractive method of synthesizing TiAl alloys. Moreover, it draws the connection between the processing, microstructure, and properties of TiAl. Thus, it identifies a step-change in tailoring the microstructural and engineering properties of the TiAl alloys, thereby providing prospects aimed at widening the applications of the alloys.

TITANIUM ALUMINIDE ALLOY SYSTEMS

Titanium aluminides are founded on the well-ordered intermetallic compound of TiAl bonded together by partial covalent bonds.[17] These types of materials have emerged as potential materials for complex structural applications that demand balanced strength and stiffness in high-temperature

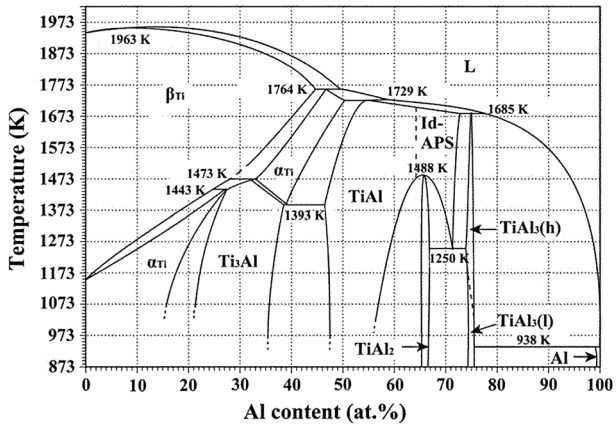

Fig. 1. Ti-Al binary phase diagram. Reprinted with permission from Ref. 42.

conditions (up to 800°C).[27] However, the major issue with these intermetallics is their brittle behavior at room temperature usually due to immobile dislocations which leads to low plastic fracture strain.[28] Consequently, the complete replacement of the heavy nickel-base superalloys has not been realized. Considerable work has been done on TiAl intermetallic compounds such as $TiAl_2$, $TiAl_3$ (trialumina), Ti_3Al (alpha 2, $\alpha 2$), and TiAl (gamma, γ),[29] as presented in Fig. 1, in efforts to develop these compounds. A review by Djanarthany et al.,[30] provides details of the constituent phases of TiAl.

Research findings ascertain that out of the number of intermetallic compounds of TiAl, only γ-TiAl or α_2-$TiAl_3$ were found to have sufficient structural application significance.[31] Recently, the near fully γ-TiAl has shown to be the most preferred for structural applications. This type of alloy comprises phases which are γ-TiAl as the major phase and α_2-Ti_3Al dispersed in various ways depending on the nature of the microstructure attained.[32] The material's microstructure is imperative as it impacts the engineering properties.[33]

According to Liu and Plucknett,[34] the near gamma ($\alpha_2 + \gamma$) phase displays mechanical properties that are more reliable for structural applications. Usually, the attained properties are a trade-off of other properties[16] and should be given principal attention when the component is intended for structural designs. To the benefit of the users, the reliance of the properties on the microstructure permits modifications of the material to be suitable for the planned application through the manipulation of process parameters. Owing to the sensitivity of the microstructure of the TiAl alloys to process conditions, TiAl binary phase diagram, as shown in Fig. 1, is beneficial to improving the process parameters[35] for obtaining the desired intermetallic phase having favorable characteristics.

Figure 1 also describes that TiAl alloys containing up to 54 at.% Al solidify via the beta or alpha phase or both phases[36] and during cooling, the

phase develops into the gamma-phase which converts into $\alpha + \gamma$ phase around 1117°C.[37] Thus, depending on processing temperatures, and composition, different microstructures can be attained to impart specific properties for specialized applications; see supplementary Figure S-1 (refer to online supplementary material). Studies also suggest the dependence of TiAl properties on starting powder grain size.[38–41] Liu et al.[41] studied the size-dependent structural properties of a Ti-48Al-2Cr-8Nb (at.%) alloy by differential scanning calorimetry (DSC) and in situ high-temperature x-ray diffractometry (XRD). They observed that with the decrease in powder particle size, the amount of the γ-TiAl phase decreased while the α_2-Ti_3Al phase increased. The evolution of α_2-Ti_3Al to the γ-TiAl phase was discovered at the temperature between 600°C and 770°C. Through the understanding of their current work, the structural features of TiAl powders are linked to their initial particle size. Thus, the basis of the characteristic of TiAl powders should be considered in improving the process parameters of TiAl alloys synthesized from powders.

Properties of Titanium Aluminide

The framework of engineering applications is constantly advancing towards the adoption of better yet affordable processes. To ensure easy transitions for pioneering developments, new and improved materials are essential for use in structural components. Titanium aluminide has the potential to satisfy the demands of the evolving engineering applications as it is lighter and stronger, has good stiffness, is less susceptible to fatigue, and has acceptable damage and is heat resistance.[43] Lighter and stronger materials conveniently yield good structural size reductions and may reduce production costs. Other important properties include creep resistance, resistance against fire, and the capacity to store hydrogen reversibly.[27,44] The combination of these properties leads to engine weight reduction which results in less fuel consumption, a considerable decrease in carbon dioxide and nitrogen oxide emissions, reduced noise[27] and an increased life cycle of the engine structure.

POWDER METALLURGICAL PROCESSING OF TIAL

The recent trend in innovative materials such as TiAl aims at ensuring excellent engineering performance and thus, compels for competitive fabrication technologies.[43,45] Previously, TiAl alloys were less considered in applications as their appealing properties were offset by poor machinability at room temperature. However, developments in the understanding of titanium aluminides microstructure, distortion mechanisms, advancements in alloying, and progress in processing technologies have led to considerable manufacturing of gamma titanium aluminide.[16] Likewise, these alloys need to satisfy complicated demands in terms of designs of structures as well as conservational and economic viability of the manufacturing technology.[46] As a result, several studies have been conducted on manufacturing titanium aluminide (TiAl) intermetallic materials through various methods. Methods such as ingot metallurgy and powder metallurgy (PM) techniques are used in industrial applications.[27] However, over the years powder metallurgy has been found to be attractive with respect to melting and casting process of ingot metallurgy identified as it is comparatively considered to be an energy-saving and time-efficient way to produce Ti-based alloys.[12–15] Popular powder metallurgy techniques include cold pressing, cold isostatic pressing, hot pressing, hot isostatic pressing, combustion synthesis, microwave sintering, spark plasma sintering, and hybrid spark plasma sintering.

Cold Pressing of TiAl

In the early research of powder metallurgy pressing of powders, several investigations involved the use of the cold press-sinter technique. In the cold pressing (CP) approach, powders are generally cold pressed in a mold and sintered in the absence of external load well above beta transus temperature to yield sintered products.[18] Figure 2 shows the illustration of the compaction method. Employed pressure can be as low as 400 MPa or as high as 1760 MPa, depending on the desired density of the green compacts.

The cold compaction and sinter technique often involves softer and irregular powders, usually in their elemental form.[47] Reports state that mixing high hardness metallic alloy such as titanium with soft metal such as aluminum yields better densities as opposed to those of hard metals only.[48]

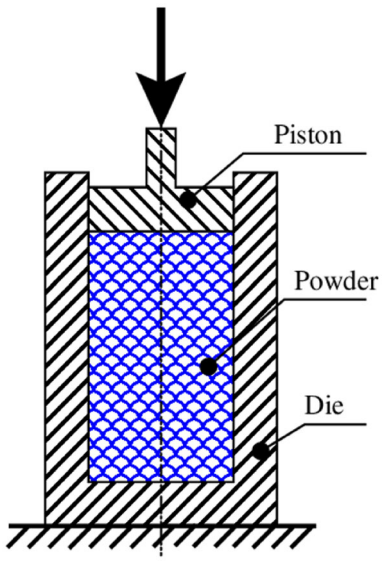

Fig. 2. Schematic illustration of cold pressing of powder. Reprinted with permission from Ref. 53.

Additionally, oxygen content in the powder particles should be at minimum levels as increased oxygen levels tend to harden the elemental powder particles thus decreasing the green density of the compacts.[49] Moreover, in titanium based-alloys, oxygen favors alpha2 stabilization and thus can alter the mechanical properties.[49,50] Consequently, the impurity content of the powder may affect the ability of CP to achieve full density by sintering. A study by Nogueira da Silva[51] produced TiAl samples through the cold compaction-sinter approach and their results showed high porosity levels and microstructure inhomogeneity which worsened with increase in Al content. The high porosity and poor microstructure limitations have caused the cold press-sinter technique to be disregarded as a viable industrial method for the production of titanium alloys.[52] Alternatively, systems such as hot pressing and hot isostatic pressing are considered as post-processing stages to increase final densities. A modified cold compaction method known as cold isostatic pressing has also been considered as an alternative cheap method to produce preforms.

Cold Isostatic Pressing of TiAl

Cold isostatic pressing (CIP) is a compaction technique utilized to produce green density compacts, particularly for larger parts not possible with cold pressing. The powder is placed and sealed in a flexible mold made from a polymer material such as urethane, rubber, or polyvinyl chloride and is then subjected to uniform hydrostatic pressure,[54] as shown in Fig. 3. The fluid in isostatic pressing is typically oil or water that produces pressure in the typical range of 400–1000 MPa.[54] Foremost, the powder is compacted to uniform density by the CIP method and later sintered in a pressure-less furnace or in a pressure-assisted furnace to increase densification. The densification process is at first governed by the yield stress of the material during which the particle plastic deformation is rapid; this is followed by the work hardening of the particles.

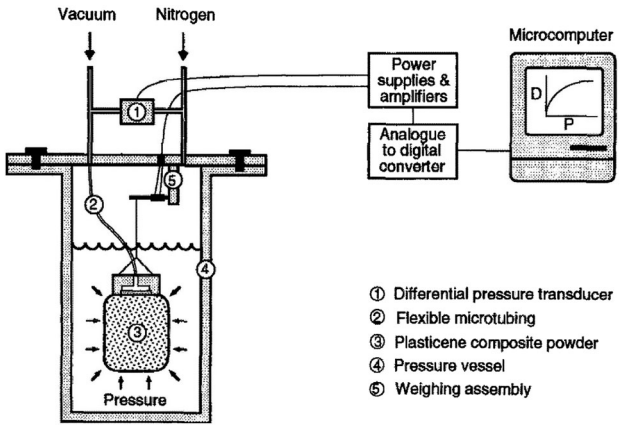

Fig. 3. A schematic diagram of the cold isostatic pressing system. Reprinted with permission from Ref. 55.

Hence, powder with high work-hardening capacity densifies more efficiently with the CIP method.

The CIP technique has limitations that involve low geometric accuracy because of the flexible mold. Another disadvantage to this method is that it requires a secondary stage of free sintering or pressure-assisted sintering. The free sintering method proves inefficient due to excessive release of heat when Ti and Al interact at high temperatures and results in volume expansion that produces the Kirkendall effect.[56] Similarly, pre-alloyed TiAl powder is difficult to sinter in the absence of pressure and pulsed current as it would require prolonged near-solidus temperature (NST) sintering to reach near full densification, which is only achievable with specialized vacuum furnace having graphite or tungsten heaters.[57] Fu et al.[58] reported high porosity content of the pressure-less sintered TiAl materials due to obtained lower green density and possibly owing to the varied diffusivities of Ti and Al, and possibly the eruption of gas bubbles that might have been entrapped during the milling process. Xia et al. obtained 60% theoretical density of TiAl using pre-alloyed gamma-TiAl, and only on addition of iron they were able to achieve about 97% theoretical density. Consequently, it is challenging to use TiAl powders to synthesize high-density γ-TiAl by the CIP-sinter approach without elemental sintering aids. Such drawbacks have led to the development of single-step pressure-assisted sintering methods.

Hot Pressing of TiAl

The hot pressing (HP) is a densification method that encompasses the concurrent application of pressure and resistance heating to the metal powder that is enclosed in a graphite die, as presented in Fig. 4. However, hot pressing techniques generally result in unsatisfactory densifications.[19] Fu et al.[58] reported porosity content of 20 vol.% of the hot pressed and heat-treated materials containing 19–35 wt.% Al and about 40% for the alloy with high Al content, which is the result of the amount of intermetallic formed. The powders were initially cold compacted using the pressure of 250 MPa. However, a study by Qian[19] suggested that a $>$ 80% pore-free density of titanium powder is obtainable at 690 MPa using the CP-sinter approach. This increased applied force may result in excessive friction during pressing which may cause inhomogeneous green-density distribution. Thus, development in the sintering processes led to the utilization of hot isostatic pressing (HIPing), which is regarded as more suited to consolidating TiAl powders[59] as compared to CP and HP.

Hot Isostatic Pressing of TiAl

The hot isostatic pressing (HIPing) process typically includes compaction of Ti-based alloy powder usually below the beta transus temperature to full

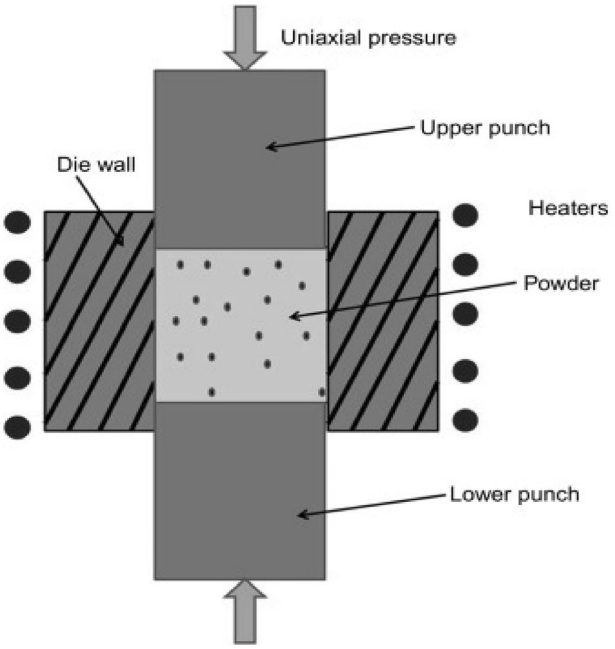

Fig. 4. Schematic illustration of the hot pressing technique. Reprinted with permission from Ref. 60.

density.[52] β-Transus temperature is sensitive to alloy composition; thus, a wide variety of microstructures can be obtained depending on whether the TiAl materials (either elemental or pre-alloyed) are processed above or below β-transus temperature.[61] In this process, a carefully shaped mold is filled with powder and HIPed under uniaxial pressure and electrical resistance heating,[62] as illustrated in Fig. 5. Once the process is completed, the mold is removed by either etching or machining.[20] This method has been utilized to consolidate powder including titanium-based alloys to high densities and good properties for use in diverse industries such as aerospace, marine, and automotive.[20,29]

For instance, Habel and McTiernan,[64] considered the impact of HIP-temperature and heat-treatment process on the microstructure and tensile properties of a Ti-46Al-2Cr-2Nb power in their study. They observed yield stresses in the as-HIP state ranged from 460 MPa to 715 MPa and ductility of 0.2–1.7%. The HIP process often results in inhomogeneous microstructure and coarsened grains as depicted in Fig. 6a, b, c, and d and often requires a heat-treatment process to optimize the microstructure; see supplementary Figure S-2 (refer to online supplementary material). Improvements of the properties were observed in this study after heat treating the alloys to attain fine duplex microstructures. Microstructure consisting of increased quantities of lamellar grains and β-phase (Fig. 6d) was reported to show improved ductility and lower strain hardening rates. These increases in lamellar colonies may be related to the high processing temperature of 1300°C. The behavior is concurrent

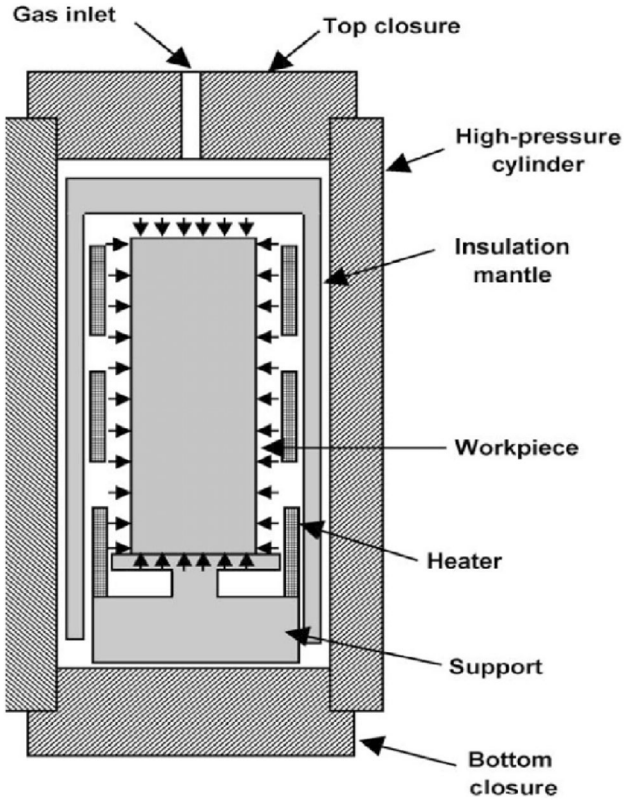

Fig. 5. Schematic illustration of hot isostatic pressing equipment. Reprinted from Ref. 63, under the term of the Creative Commons CC BY license.

to the expected microstructural evolution based on the Ti-Al phase diagram in Fig. 1. After heat treatment of alloys with Al compositions in the range of 45–48 at.% at temperatures of 1300–1500°C, the microstructure is predominantly nearly lamellar and fully lamellar structure above the α-transus line.[16]

The aim of HP/HIP is to produce fully dense components, and several successes are widely documented,[18] including the studies on TiAl.[65,66] However, the disadvantage of the HP/HIP processes is the long processing time, resulting in the inherent scattering of properties. Moreover, the production of complex geometry using HP/HIP is not easy and often requires several steps before processing of the materials, which generally include 2D and 3D modeling for capsule design and densification and shrinkage during HIP as well as software development for NC milling.[67] The main drive in titanium alloy processing is to produce a refined, homogeneous, and isotropic microstructure irrespective of the titanium alloy composition used.[18] Therefore, the long processing HP/HIP is being replaced by rapid sintering techniques to achieve improved property levels.[65]

Combustion Synthesis of TiAl

Combustion synthesis involves the manufacture of products from reactants through a solid-state

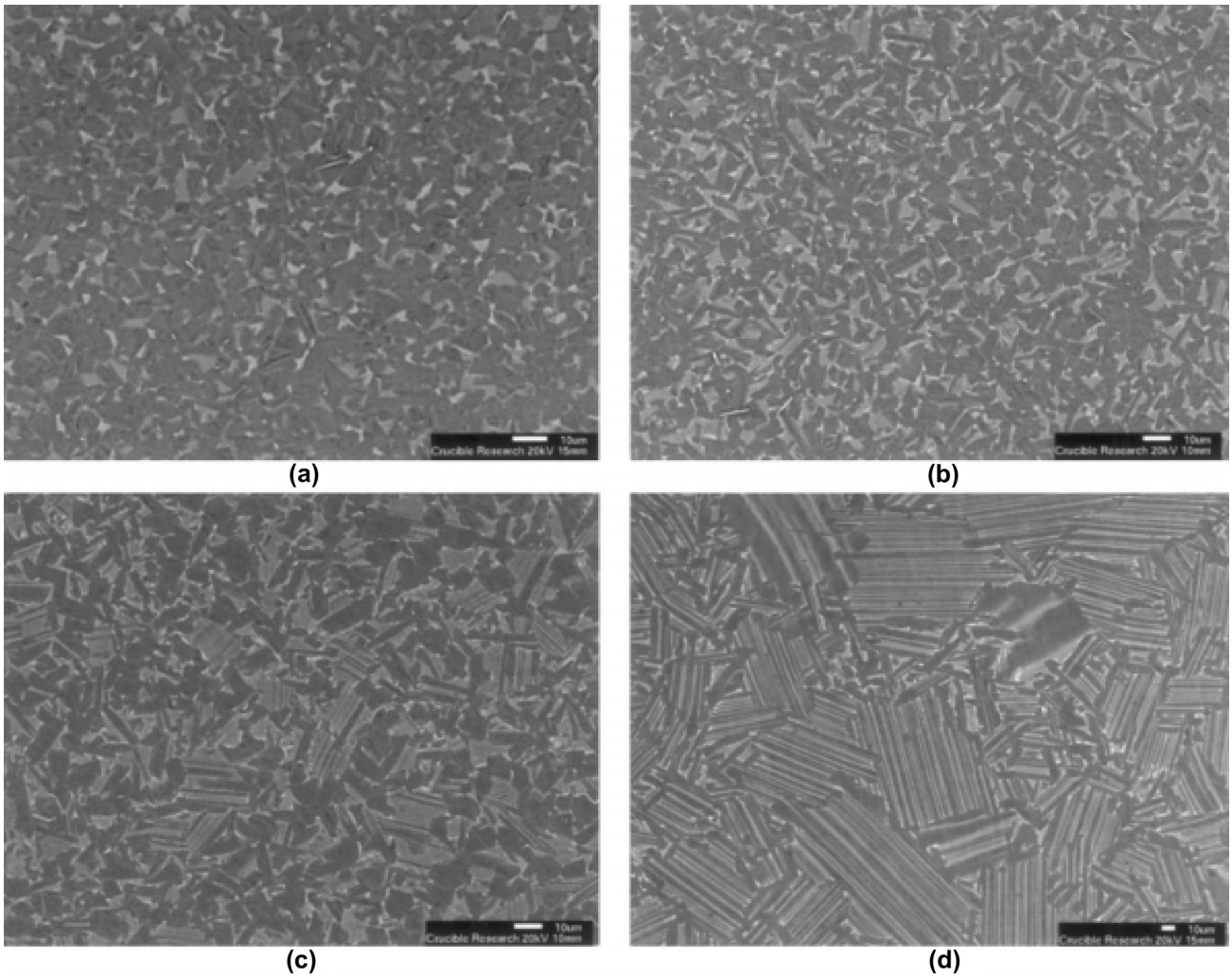

Fig. 6. Backscattered electron image of microstructures of Ti-46Al-2Cr-2Nb synthesized by HIP process, the α_2-phase appears light gray, the β-phase white. HIP temperatures; (a) 1200°C; (b) 1240°C; (c) 1270°C; (d) 1300°C. Reprinted with permission from Ref. 64.

process in which the reactants are self-sustaining through the exothermic heat of a reaction. Typically, sufficient exothermic heat is released when the threshold activation energy is surpassed, thus initiating the reaction to self-propagate inside a powder mix.[68] This method can be performed in either the self-propagating high-temperature synthesis or the thermal explosion approach. The benefits of combustion synthesis include energy-saving, ease of operation, rapidity of the process, and formation of pure products that emanate from the release of volatile impurities at high temperatures.[69] However, the products are highly porous due to this volatilization as well as volume disparity between reactants and products.

Self-Propagating, High-Temperature Synthesis of TiAl

In a conventional self-propagating high-temperature synthesis (SHS) process (Fig. 7), the powder constituents are dry-mixed and cold-pressed to

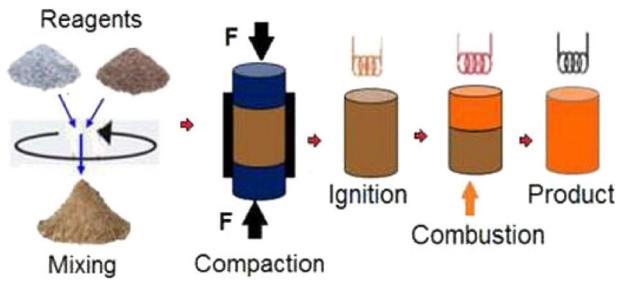

Fig. 7. Self-propagating high-temperature synthesis process. Reprinted from Ref. 72, under the terms of the Creative Commons CC BY license.

obtain a green compact.[69,70] The green compact is then placed in an SHS device under a controlled environment and kindled either by an electrically heated coil, laser beam, or electric discharge.[70] Thereafter, the green compact reacts and releases adequate heat that travels along the entire volume of reactants converting them into products.[71] If the total heat distributed to the volume of the material

is less than the heat released from the reaction, the ignition of material and self-sustaining synthesis will not be possible.[68,70] For the material to be ignited successfully, it must have adequate thermal conductivity to enable the required temperature gradient and that can be determined by this formula:[68]

$$(-\Delta H)k_i(T_i,\eta) > \frac{1\partial}{r^2\partial r}\left[r^2\lambda_e\frac{\partial T}{\partial r}\right]_{t_i} \quad (1)$$

where T_i and t_i are, respectively, the temperature and the time of ignition, η is the degree of reaction evolution, ΔH is the reaction enthalpy, ΔH is the enthalpy of the (exothermic) reaction [J/mol], k_i is the constant of reaction rate at ignition temperature [mol/m^3/s], λ_e is an operative thermal conductivity of the starting powder mix, and r is the radial position. From the equation, it is clear that ignition of powder materials is favored by high ΔH (≥ 100 kJ/mol) and high k_i.

Several studies have reported SHS of various materials particularly the intermetallic compounds and their composites.[73] Nickel-based intermetallics are among those broadly investigated.[74,75] However, not many studies have been conducted on the SHS of intermetallics of titanium, especially titanium aluminides. Mainly because the combustion synthesis of TiAl in the self-propagating mode is frequently confronted with difficulties due to the low enthalpy variations of the exothermic reactions between aluminum and titanium. Production of TiAl by SHS mode creates an adiabatic temperature of about 1245°C in the system, which is less than the required minimum of 1527°C for the reaction to become self-sustaining.[69] Consequently, researchers studied various approaches to effectively produce TiAl via SHS mode.

Vershinnikov and Borovinskaya[76] investigated the influence of charge composition, stoichiometric ratio, and additives on particle size, morphology, and phase formation. They used powder particles that varied from 100 μm (fragments) to 3–4 μm (plates) and 500 nm (powders). A polyphase artifact containing TiAl, Ti, Ti_3Al, Ti_2Al, and spinel $MgAl_2O_4$ was achieved by synthesis at low temperatures and with an aluminum shortage. The authors were successful to achieve a sufficient adiabatic temperature in the SHS process by use of magnesium perchlorate and calcium peroxide which increased the combustion rate and temperature. An increase in magnesium resulted in a significant fine intermetallic Ti_2Al phase.

Farley et al.[71] synthesized metallic foams utilizing an SHS reaction fabricating a porous alloy. A mixture composed of nanoscale particles of titanium and aluminum was passivated with a gasifying agent (perfluoroalkyl carboxylic acid or polytetrafluoroethylene) and pressed into pellets which were then kindled with a laser. Through the use of nanoparticles, TiAl alloy that has a porous structure was obtained, an achievement not possible on a micron-scale as the Ti-Al mixture would not self-propagate without the aid of an external heating source. Nanostructured particles have reduced melting temperatures, which is said to result from an increase in specific heat and a decrease in the melting entropy and enthalpy as the particle size decrease[77] reduced ignition sensitivity, greater surface energy compared to conventional bulk materials because of the vast surface-to-volume ration, and better absorption properties when compared to micro-scale particles;[78,79] thus, Ti-Al nanoparticle composites can self-sustain a reaction on ignition. However, the thermodynamic properties of nanostructured materials are also influenced by the particles shape and the material's crystal structure.[80] Thus, the degree of the size-dependent thermodynamic properties is specific to the nature of the materials.

Adeli et al.[69] studied SHS of titanium aluminides for different Ti:Al atomic ratios. Powder mixtures were pressed and the compacts were simultaneously and rapidly preheated and ignited by induction heating causing the compacts to sustain a reaction and also avoid precipitation of undesired phases. X-ray diffraction analyses revealed that the main product constituents were TiAl, Ti_3Al, and $TiAl_3$ with relative density in the range of 60–70% with an increase in combustion temperature, as displayed in Fig. 8. Increasing aluminum content results in the increase of combustion temperature as more aluminum melt reacts with titanium releasing excessive exothermic heat of reaction, which is directly related to the adiabatic temperature and thus the combustion temperatures.

Other research work in SHS of TiAl includes studies by Sohn and Wang[81] involving the synthesis of TiAl through the SHS process by ignition of compacts using a silicon carbide heating component. $TiAl_3$ was accomplished from a Ti-75at.% Al powder mixture; however, mixtures with lower Al content such as Ti-50%Al and Ti-25%Al yielded products having minor quantities of other phases such as Ti_3Al and $TiAl_2$. Medda et al.[82] synthesized pure $TiAl_3$ product via a combination of mechanical

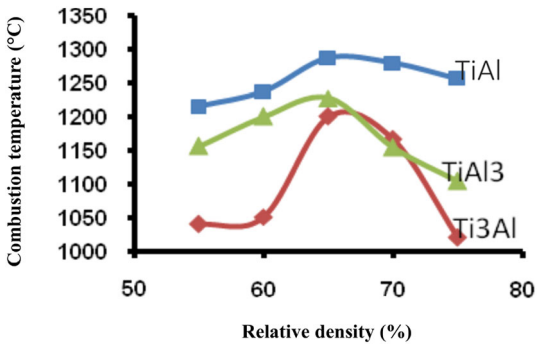

Fig. 8. The effect of compact density on combustion temperature. Reprinted from Ref. 69, under the terms of the Creative Commons CC BY license.

activation and SHS, using a tungsten coil to ignite both loose and compacted pre-activated powders. The success in the synthesis of $TiAl_3$ was reasoned to be because of the mechanical activation step which encouraged chemical reactivity of the powders enabling the reaction to be self-sustainable. Orru et al.[83] successfully synthesized Ti_3Al and TiAl through field-activated combustion using an ignition heat source in the form of a tungsten coil and studied the influence of an external electric field on the combustion front and the composition of the product. They discovered that increasing the electric field strength enhanced the initiation and spread of the combustion reaction and resulted in a pure product.

Thermal Explosion of TiAl

Thermal explosion (TE) involves a powder mixture being ignited at a constant heating rate and the reaction dissipates throughout the volume of the sample, therefore avoiding cracking and deformation behavior caused by uneven heating. A common practice in TE mode is to preheat the reactants before ignition or to heat the reactants to a point where the reactions take place over the entire sample.[69,73] Contrarily, in SHS mode the compacted powder mixture is heated up in a furnace until the onset of the reaction between the reactants and the reaction then propagates until it reaches steady-state conditions. However, with weakly exothermal mixtures the propagation deviates from a non-steady state to a spin or oscillatory motion. To overcome this instability of the propagation front, TE is frequently employed in which the weaker exothermal mixture is enclosed by an extremely exothermal mixture thereby causing the weaker exothermal reaction to successfully react to form products.[84]

Jiao et al.[85] synthesized pure $TiAl_3$ intermetallics with a porosity of 55.4% from Ti-75 at.% Al elemental powder mixtures using the TE method. Microstructural investigation using back-scattered

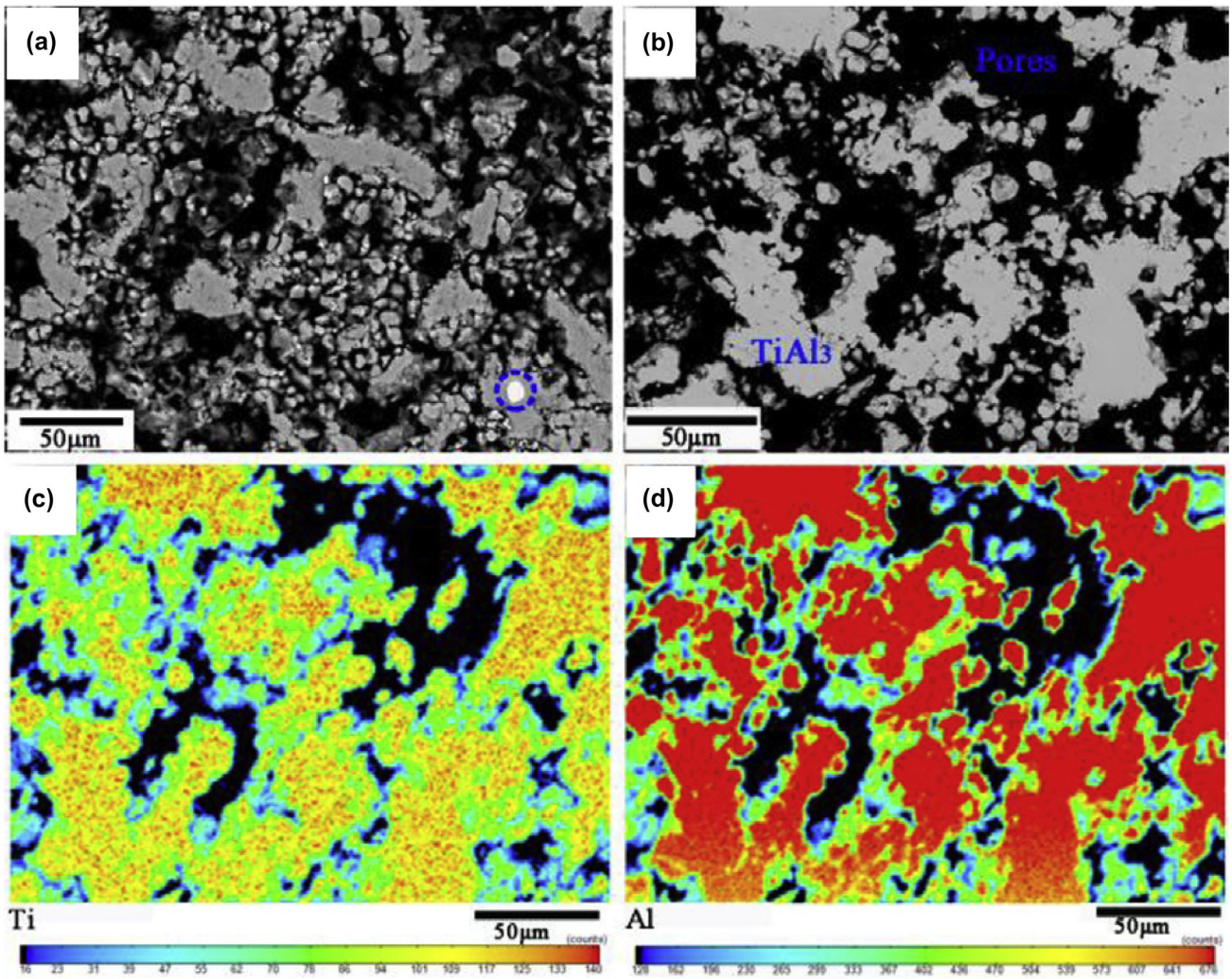

Fig. 9. BSE images of TiAl alloy sintered at (a) 700°C and (b) 1000°C and their elemental color mapping images (c and d, respectively). Reprinted with permission from Ref. 85.

electron (BSE) on samples sintered at 700°C and 1000°C, and their elemental color mapping images for Ti and Al, in Fig. 9a, b, c, and d, revealed that the gray zone was intermetallic phase whereas the dark areas indicated pores in a and b. It was deduced in the study that pores formed and interlinked among the uniform $TiAl_3$ skeletons because of the strong TE reaction. They also discovered that $TiAl_3$ layers contained a few unreacted Ti particles encircled with blue dots in Fig. 9a and deduced that it occurred because of a rapid exothermic reaction. A porous product presenting a homogeneous composition of $TiAl_3$ with uniformly distributed Ti and Al elements was achieved at 1000°C. Thus, a higher sintering temperature or longer holding time is essential to synthesize the homogeneous single $TiAl_3$ products.

Lagos et al.[86] proposed a combustion process for the production of well-densified gamma-TiAl alloys with improved microstructure and mechanical properties. This process consists of multiple stages and involves TE and compaction in which the metallic powders are heated up until they reach ignition temperature. The ignited compacts start to react throughout the sample volume, and upon completion of the reaction, the mechanical load is applied. Finally, thermal treatment is applied to the samples to obtain the desired microstructure and to reduce interior stresses. They studied the effect of some parameters of the thermal explosion + compaction process on the microstructure. Results showed that applying pressure at an earlier stage and the use of a higher temperature (1200°C instead of 900°C) lead to a substantial increase in the product density and improvement of the microstructure.

Thermal explosion, as well as the self-propagating high-temperature combustion methods, has shown some level of success in consolidating TiAl compounds. These approaches, however, are not sought after because of the formation of unwanted phases. On the other hand, preheating of the compacted powders before ignition cannot be easily performed because of the high reactivity of titanium and aluminum. The deficiency of these synthesis methods led to finding alternative methods to efficiently manufacture TiAl products.

Microwave Sintering of TiAl

Microwave (MW) energy is an electromagnetic radiation method with a frequency in the range of 300 MHz to 300 GHz and an associated wavelength of 0.01–1 m. Microwave technology offers an opportunity at synthesizing materials utilizing electromagnetic radiation that produces high temperatures and enables densification of materials with a reduced processing time.[87] The short sintering time signifies that consolidation of materials can be achieved with lower energy consumption.[88] Furthermore, the rapidity of this process also means that materials with finer and homogeneous microstructure may be obtained and therefore, result in enhanced mechanical properties. In microwave sintering, the sample is heated at the core by absorbed radiation and the heat is then transferred from the sample core to the entire volume of the sample.[89] So far, microwave heating has been limited to ceramics, refractory materials, and ferrites due to challenges encountered with microwave sintering of bulk metal-based materials.[90] The challenges arise because of the high conductivity of metals which prevents the internal development of the electric field as these materials have limited penetration of MW radiation as they readily reflect the incident waves.[91]

Efforts in studies on the MW sinterability of metal have shown that powdered metals can be consolidated using MW heating.[90,92,93] However, scholars have reported on the inefficiency of MW radiation in heating titanium powder,[94,95] and this behavior is attributed to the paramagnetic nature of the Ti metal.[94] To the knowledge of the authors, there is currently insufficient or no literature available on the use of MW radiation for sintering of TiAl alloys. The limited use of MW energy for powder metals, alloys, and some ceramics could be associated with challenges arising when intending on heating green compacts to a high temperature with microwave energy alone. Due to the nature of the inverse temperature profile resulting from the specimen absorbing microwave energy, the specimen will be at a higher temperature than the environment, resulting in a temperature gradient within the specimen making them more susceptible to thermal shock.[96] Investigation into the unfavorable heating conditions in microwave sintering has led to the development of using hybrid heating also known as bi-directional heating to avoid temperature gradient and thermal shocks.

Microwave Hybrid Heating (Two-directional Microwave Heating) of TiAl

The principles of microwave hybrid heating involve the utilization of materials having a higher dielectric loss factor to impart directional microwave heating;[97] a diagram of hybrid microwave sintering is shown in Fig. 10. These materials are known as susceptors and absorb microwaves at low temperatures and accumulate heat, which is then conventionally transferred to the sample.[89,96] Susceptors function as a microwave-coupled external heating source and heat the powder compacts from the surface while the internal part is being heated by the absorbed microwave; see supplementary Fig. S-3 (refer to online supplementary material). The combined heating modes ensure that heat is distributed evenly throughout the volume of the specimen. This uniform thermal gradient favors the uniform properties of the materials.

Several studies reported success in synthesizing TiAl products by use of titanium hydride (TiH_2) susceptor through microwave technique.[89,99,100]

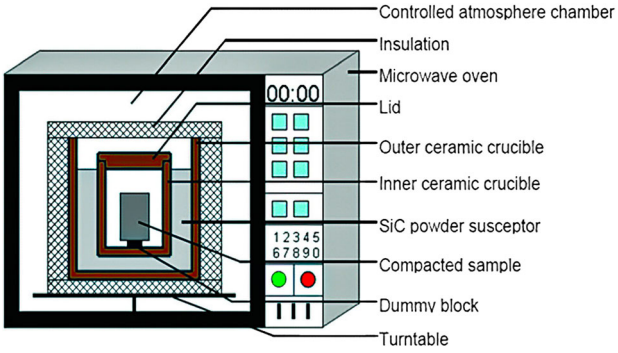

Fig. 10. Schematic of bi-directional (hybrid) microwave sintering. Reprinted from Ref. 98, under the terms of the Creative Commons CC BY license.

TiH_2 decomposes to form Ti atoms that react with the constituents of the powder mix. The presence of TiH_2 encourages a rapid heating rate and consequently protects the reactive powders against oxidation due to reduced reaction time and it also encourages the formation of pure products. The use of MW susceptor has proven efficient in improving paramagnetic Ti response to MW radiation.[101]

Investigation into microwave sintering (direct and hybrid mode) of Ti-based alloys is relatively new.[89] Though TiH_2 was demonstrated to be an effective MW susceptor in sintering Ti-based alloys such as TiAl,[89,99,100] the existing data are relatively insufficient and the influence of the processing conditions on the mechanical behavior of the sintered alloys is not widely studied. Further research into the application of microwave sintering of Ti-based alloys will afford a better understanding of this method to produce Ti-based artifacts and their processing behavior and microstructural and mechanical properties. Bridging this information gap will enable wider use of the microwave sintering system.

Spark Plasma Sintering of Titanium Aluminide

The novel spark plasma sintering (SPS) technique was developed as a viable method for sintering TiAl products with desired properties.[62] SPS has the advantage of using lower sintering temperatures and shorter holding times as compared to pressureless sintering and hot pressing.[102] These characteristics of SPS are desirable for limiting grain growth.[13,15,43,103,104] Additionally, SPS is capable of processing materials with high melting points and limited ductility into profiles previously unachievable.[105] Specimens produced through SPS have demonstrated improved microstructural and physical properties.[13,103]

As previously discussed in Mphahlele et al.,[106] the SPS technique (as shown in Fig. 11) employs a low voltage pulsed current that dissipates through powder samples in an electrically conducting die, and the powder is coalesced by the concurrent

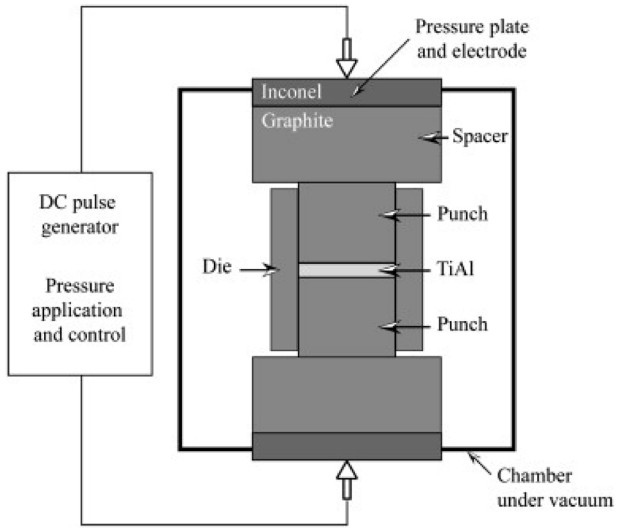

Fig. 11. Spark plasma sintering schematic. Reprinted with permission from Ref. 5.

action of the electric current and uniaxial pressure.[62] According to Olevsky and Dudina,[107] the synthesizing process is generally versatile. The pressure could go up to 150 MPa with graphite tools,[103] and superposition of high AC and DC currents typically from 1 kA/m^2 to 10 kA/m^2 produced by a low voltage of about 10 V is applied to the whole set-up. Generally, heating rates up to 1000°C/min are attainable depending on the profile of the dies and punches. Cooling rate up to 150°C/min is attainable under vacuum conditions and can go as high as 400°C/min under gas flow.[25] Thus, the correct selections of the employed pressure and the pulse current constraints such as amplitude, time, and the pause between pulses are essential for successful sintering using SPS technology.

As the global interest increasingly advances towards developing materials with exceptional properties by taking advantage of the benefits of the SPS process, focus on advanced materials such as TiAl has increased exponentially in recent years.[18] The spike in interest is due to the favorable characteristics of TiAl as discussed in the previous sections. Efforts were made to investigate several factors influencing the relative densities, microstructure, and physical properties of the TiAl produced by the SPS method.

In the studies by Matsugi et al.[108] and Wang et al.,[109] a comparative effect of temperature and pressure on densification of TiAl alloys using SPS can be made. Matsugi et al. reported relative densities of 3.56–3.71 g/cm^3 for samples sintered at 1300–1400°C under an applied pressure of 18.9–33 MPa as provided in Table I. While in the study by Wang et al., they achieved relative densities in the rage of 3.944–3.967 g/cm^3 for the sintering temperatures of 1050–1250°C and applied pressure of 50 MPa, as shown in Table II. However, their study showed that lower temperature of 900°C was

Table I. SPS conditions and properties of the SPSed TiAl samples. Reprinted with permission from Ref. 108

	Resistance sintering conditions			Average grain sizes (μm)				
Specimen	Temperature (K)	Time (ks)	Applied pressure (MPa)	Core	Lamellar	Equiaxed grains	Density × 10^3 (kg m^3)	Area fraction of lamellar (%)
No. 1	1573	0.9	18.9	30	30	14	3.56	–
No. 2	1623	0.9	18.9	22	23	17	3.59	–
No. 3	1648	0.9	18.9	22	27	16	3.57	–
No. 4	1673	0.9	18.9	–	29	23	3.70	16.4
No. 5	1673	0.9	33.0	–	28	21	3.71	11.6
No. 6	1673	1.8	18.9	–	26	25	3.71	6.0

Table II. Density and hardness of SPS TiAl samples at different sintering conditions. Adapted from Ref. 109, under the terms of the Creative Commons BY license

Temperature (°C)	Applied pressure (MPa)	Density (g cm^3)	Hardness (HV)
900	50	3.392	278.6
1050	50	3.944	413.0
1100	50	3.966	420.0
1150	10	3.947	–
1150	30	3.961	–
1150	50	3.967	417.0
1250	50	3.965	430.0

inadequate to achieve good density. Although lower temperatures may be beneficial for limiting grain growth due to reduced grain-boundary atomic diffusion, high temperatures encourage additional plastic deformation and leads to rapid densification of the samples.[25,110] Thus, when the temperature was increased to 1150°C, their results showed improved densification even for sample synthesized using low pressure of 10 MPa. When they increased pressure to 30 MPa and 50 MPa for the same temperature of 1150°C, an increase in the relative densities of the samples was observed. Aldoshan[111] reported on similar observation in which high densities of about 3.95 g/cm^3 was achieved at a temperature of 1100°C and applied pressure of 50 MPa. The reported high densities in the study by Wang et al. and Aldoshan were attributed to the high uniaxial pressure used in the study that enabled the high densification of the TiAl samples at comparatively low temperatures to those employed in the study by Matsugi et. al. This was achieved because high pressure disintegrates powder agglomerates and encourages contact between particles, therefore, eliminating voids and increasing the densities of the samples.[25,112]

Molénat[113] conducted sintering on a Ti-44Al-2Nb-2Cr-1B (at.%) powder. The temperature of 1190°C and 1225°C and a pressure of 100 MPa with a holding time of 2 min were used in their study. Samples sintered at both 1190°C and 1225°C showed a similar fine-grained homogeneous duplex microstructure comprising lamellar colonies and γ-phase grains observed under a scanning electron microscope (SEM) as presented in Fig. 12a. The lamellar structure is associated with thin lamellae of ordered α_2 Ti_3Al-phase or γ TiAl-phase. The author further conducted a tensile test on the sample sintered at 1190°C, and the result showed high ductility of up to 1.95% and high yield stress of up to 737 MPa as shown in Fig. 12b. A similar microstructure obtained within a temperature range of 35°C indicates the effectiveness of the SPS technique in consolidating TiAl alloys.

The study by Couret et al. (2008)[5] presented further details on the microstructural features of SPS Ti49-Al47-Cr2-Nb2 alloys in terms of fractography. The alloys were sintered in the temperature range of 1100–1225°C. The fracture morphology of the distorted TiAl sample sintered at 1100°C is exhibited in Fig. 13a, b, and c. These SEM images show a sample with only a restricted amount of microcracks as revealed in Fig. 13c. The authors observed that areas associated with fracture initiation as shown in Fig. 13a did not show any cause of failure. They assume that failure in the materials resulted because of defects such as larger particles or inclusions in the powder, mainly because the materials presented high relative densities and ultimately insignificant pore stress raisers.

Xiao et al.[114] considered the influence of SPS temperature on the evolution of the microstructure and engineering properties of the Ti-47%Al alloy.

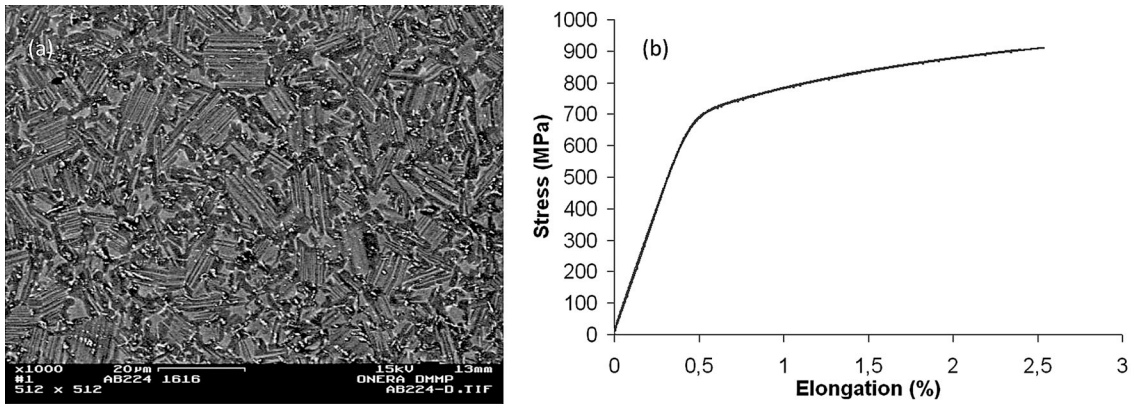

Fig. 12. (a) SEM image of the TiAl alloy surface, (b) Tensile curve for samples sintered at 1190°C. Reprinted with permission from Ref. 113.

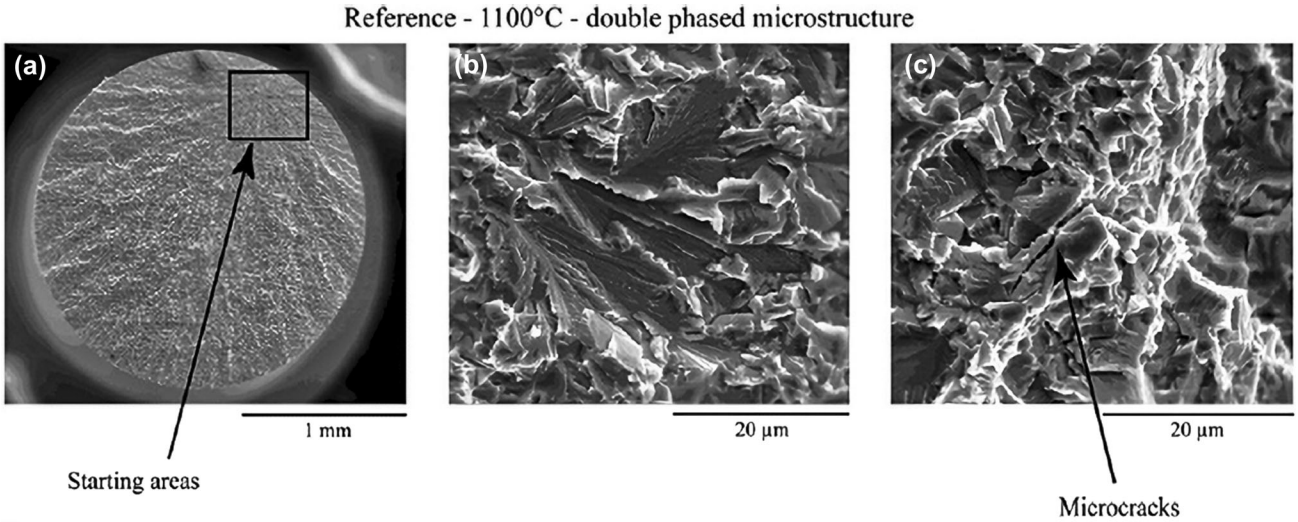

Fig. 13. SEM micrographs of the fracture surface of the TiAl alloy distorted in tension at ambient temperature. Reprinted with permission from Ref. 5.

This was achievable using x-ray diffractometry (XRD), SEM, and mechanical testing. The data obtained from their study indicated that the primary phase was TiAl and only limited phases of Ti_3Al and Ti_2Al were detected in the SPS samples. They also observed that samples sintered at 1000°C consisted of equiaxed grain of 100–250 nm size and demonstrated compressive strength of about 2013 MPa and a bending strength of 896 MPa. However, at high temperatures, they observed a coarsened equiaxed TiAl phase and lamellar Ti_3Al phase that resulted in reduced compressive strength to about 1990 MPa and bending strength to about 705 MPa. The authors also observed a higher micro-hardness with samples sintered at 1000°C than that of the samples sintered at 1100°C. These observations suggest that the micro-hardness and compression strength are influenced by the grain size distribution of TiAl alloy and the behavior correlates to the Hall–Petch relationship between strength and grain size. With the SPS temperature increase, the effect of grain coarsening on strength is more significant.

Wang et al.[115] focused on understanding the microstructural evolution by studying the densification mechanisms of Ti-45Al-7Nb-0.3W alloy during the sintering process. Their results showed that α and γ precipitates form in the early stage of sintering with only fragments of the residual β phases. During the SPS course, they observed that there was a formation of the α_2/γ lamellar colonies at the edge of the α and γ precipitation zone, development of the α_2 phase and β phase with B_2 structure, as well as dynamically recrystallized γ grains (Fig. 14a, b, and c). This is possibly because in the sequential stages of sintering, densification is governed by the development of sintering necks controlled by diffusion and the pore closure. Furthermore, since Ti and Al have a great difference in their melting point, significant segregation occurs during solidification of the powder particles; partial melting of the alloy is innate and likely to

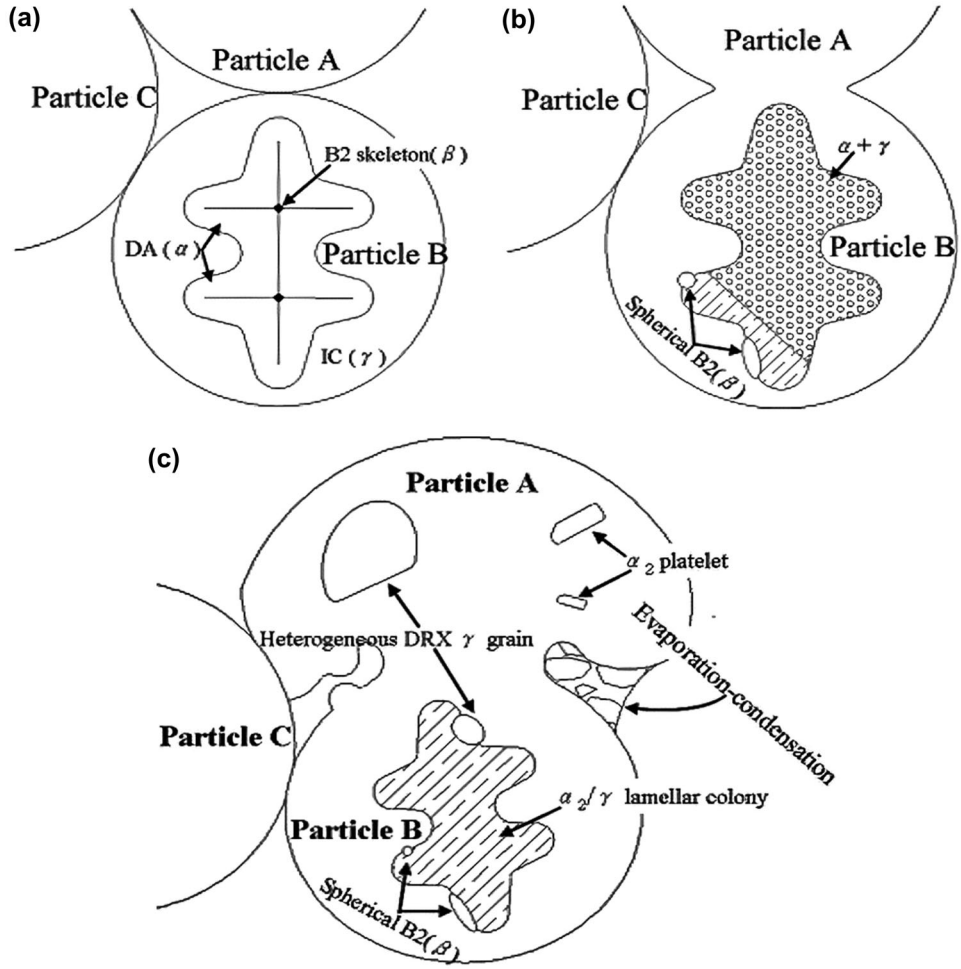

Fig. 14. Illustration of step-wise microstructure evolution during the SPS densification: (a) dendrite in the as-atomized powder; (b) primary phase of densification; (c) later phase of densification. Reprinted with permission from Ref. 115.

result in surface swelling between adjoined particles which contributes to densification mechanisms. On the other hand, consolidation of pre-alloyed TiAl is performed in the solid-state form; thus, densification is mainly controlled by solid-state grain boundary diffusion.[111]

Trzaska[14] also investigated the mechanisms involved during the densification of TiAl (Ti48.7Al47.3Cr1.9Nb2 at.%) powder by the SPS technique. In their study, the densification was observed to occur from 800°C to 1300°C as shown in Fig. 15a. They reported that the densification of the TiAl was influenced by distortion of the powder particles occurring by microscopic elasticity mechanisms and recovery recrystallization phenomena; see supplementary Figure S-4 for proofs of recrystallized grain and contacts between two particles (refer to online supplementary material). The distortion is said to occur by power-law creep given by;

$$\dot{D} = 5.3\left(D^2 D_0\right)^{1/3} \frac{1}{\sqrt{3}} \left(\frac{D - D_0}{1 - D_0}\right)^{1/2} \dot{\bar{\varepsilon}} \qquad (2)$$

with D_0 being the primary relative density, $\dot{\bar{\varepsilon}}$ is the corresponding (Von Mises) powder particle distortion rate, and $\dot{D}$ is the densification rate. Subsequently, a corresponding strain rate ($d\varepsilon/dt$) was determined to be about 10^{-3} s^{-1} (consistent with glide and climb dislocation mechanisms) and remained constant over densification interval for $0.65 \le D \le 0.95$ as shown in Fig. 15b. Their study revealed that the densification of TiAl by SPS occurs through high-temperature metallurgical mechanisms, which include glide and climb dislocation movement mechanisms, dynamic recovery mechanisms especially in the sub-boundaries, and recrystallization mechanisms.–

The role of sintering neck growth and the pore closure in the densification of the TiAl alloy (Ti-45Al-5Nb-0.2B-0.2C, at.%) can be noticed in the study by Bambach et al.[116] In their study, the sintering process was performed in a vacuum at a sintering temperature of 1250°C for 4 min and under a load of 35 MPa. Through electron

backscatter diffraction (EBSD) analysis, they observed that the microstructure formed during SPS reveals that the powder particles deform and bond together as shown in Fig. 16a. Although the boundary of the starting powder particles was still distinct, the SPSed specimens showed no visible porosity, which is evident in Fig. 16b, signifying a successful powder synthesis during SPS. Their SPSed alloy showed a homogeneous equiaxed microstructure containing globular α-phase (white) and γ-phase (gray) according to the different backscattering contrast. The evolved microstructure is typical of the conventional γ-TiAl where the solidification procedure occurs in the absence of β stabilizing (Mo, Cr, Mn, V, Nb) elements and a lower Al concentration (42–44%).[117]

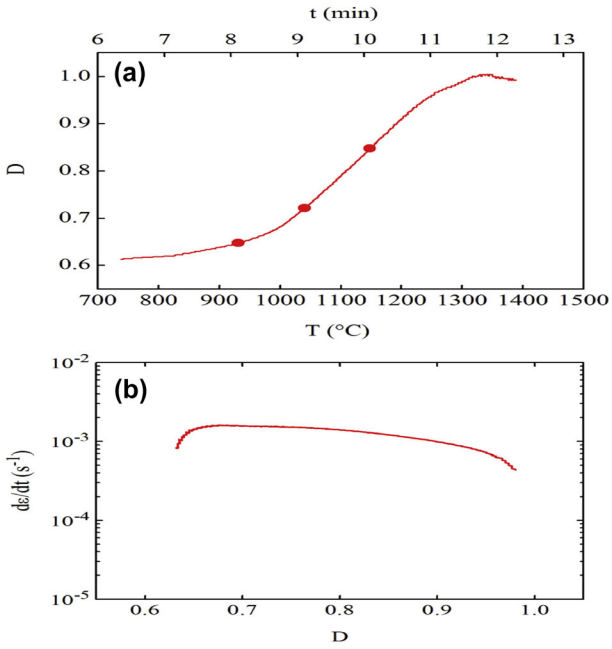

Fig. 15. Initial SPS cycle data of (a) relative density D as a function of temperature T and time (t = 0). The points on the curve show the intermittent states studied. (b) Corresponding powder particles distortion rate function of sample relative density. Reprinted with permission from Ref. 14.

Xia et al.[118] were successful in achieving near-full densification of Ti-48Al-2Cr-2Nb alloy powder by SPS at 1100°C for 4 min under the load of 80 MPa. However, the author observed that the successful synthesis by SPS was accompanied by an unpredicted phase consisting of oxygen- and carbon-enriched γ-Ti and chromium-enriched β-Ti in the as-sintered TiAl alloy. Development of this unexpected phase was credited to local overheating owing to a high density of current transmitting through the narrow intersection between particles. The observation indicated that while SPS is an effective consolidation method, it can lead to inhomogeneous microstructure for TiAl alloy powder because of the local overheating. The overheating problem can be associated with the traditional SPS tooling configuration which is represented by a conical transition between punches and spacer. To avoid overheating, a configuration that involves using disk-shaped transitional spacers of different thicknesses and diameters can be considered in place of the conical transition.[119]

Gu et al.[120] studied the effect of sintering temperature on the microstructure and mechanical properties. In their study, Ti-43Al-5Nb-2V-1Y powders were sintered at varying temperatures between 1100°C and 1250°C and a load of 40 MPa. The scanning and transmission electron microscopy analyses of the sintered samples showed duplex, nearly lamellar, and fully lamellar microstructures were attained because of the sintering temperature. They observed that the high sintering temperature led to grain coarsening and extensive segregation of the YAl_2 phases, which resulted in the deterioration of the mechanical properties of the alloy. The observed effect could be a consequence of activities of vacancy diffusion as it greatly affects precipitates

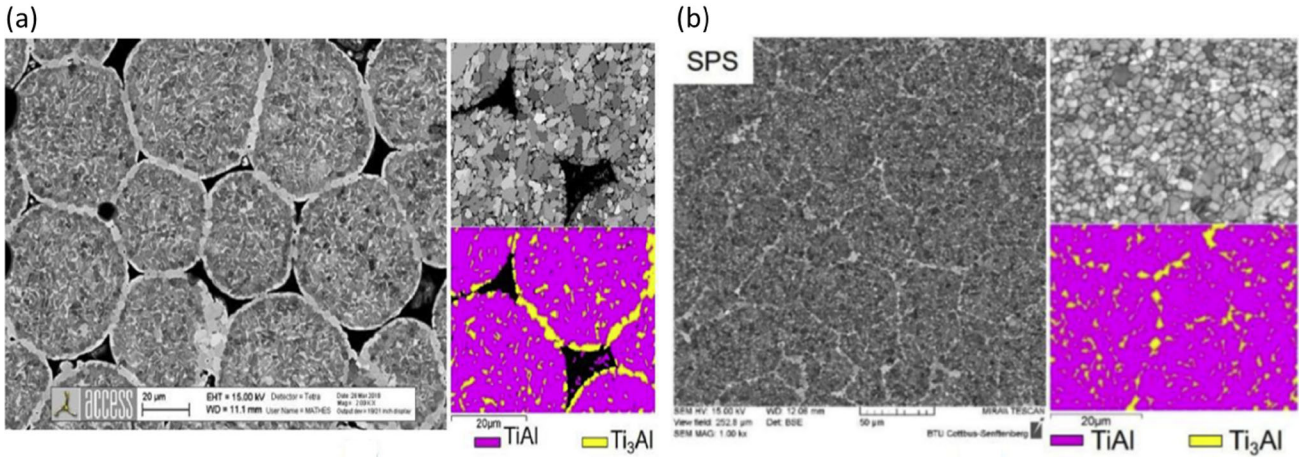

Fig. 16. BSE-SEM image and conforming EBSD pattern and phase maps (a) of powder particles of the TiAl alloy subjected to the SPS process at nominal load, (b) after SPS. Reprinted with permission from Ref. 116.

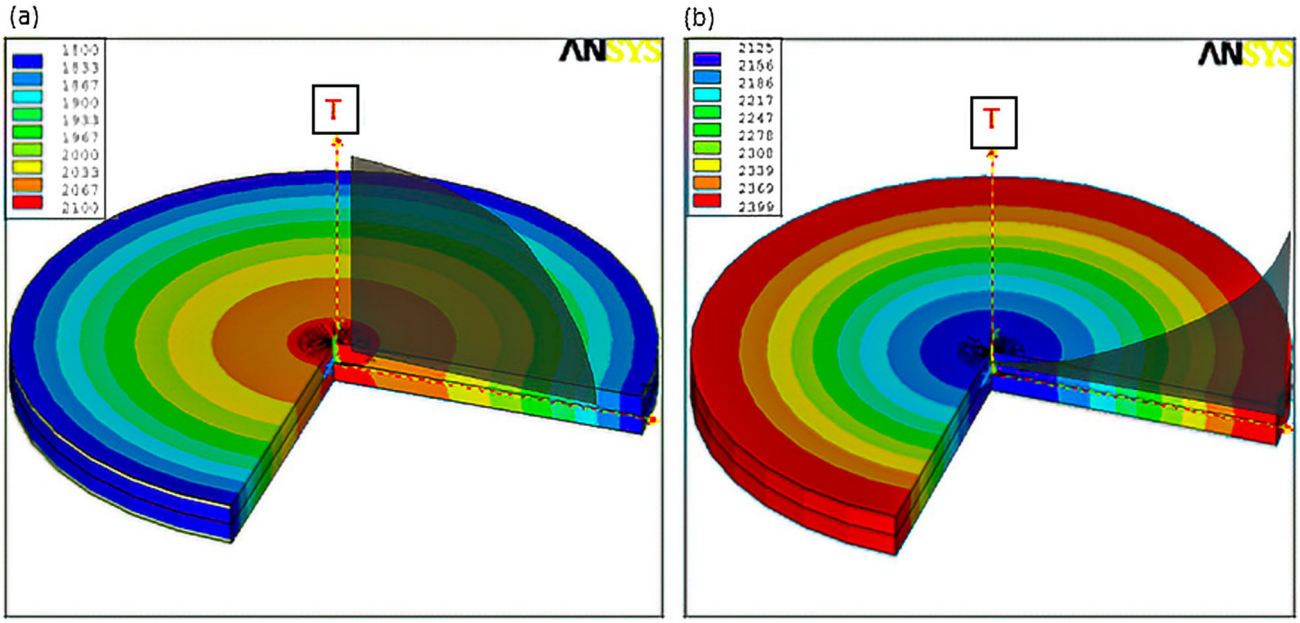

Fig. 17. Thermal gradients in a large disk sintered in (a) SPS and (b) HIP. Reprinted with permission from Ref. 129.

kinetics which is also associated with temperature.[121]

Hybrid-Spark Plasma Sintering: outlook for fabricating TiAl

The industrial era of manufacturing processes has since shown rapid development, which demands constant improvement of the existing processes and practices. Such rapid changes have caused companies to be more competitive and set out new goals in industrial processes. Consequently, companies have looked with renovated interest towards the introduction of innovative technologies and careful consideration towards an immense expansion of the size and scale of industrial production.[45]

Despite SPS being favored as an effective technique for fast sintering owing to the fast heating rates and the combination of low temperature and pressure, there is universal agreement that it can manufacture products with enhanced properties compared with traditional systems such as hot isostatic pressing;[122] the operation is limited when considering the size of products.[123] Previously, SPS has been used solely for producing simple disc specimens of sizes ranging from 10 mm to 40 mm.[122,124] Recently, scholars have attempted processing larger specimens and near-net shape parts using SPS.[13,125,126] Voisin et al.[126] demonstrated success to produce an 80-mm-long TiAl near-net shape blade using SPS. The results of their SEM analysis on the cross-section of the blade displayed homogeneous microstructure at different parts of the blade. This success could be linked to the complex tooling setup which includes near-net shape punches with different height adjustments and semi-cylindrical pieces to give its shape to the blade and ensure even heat distribution to the parts regardless of the shape anomalies. Additionally, the authors used FEM simulations in predicting conditions for successful sintering of the parts. This success represents the versatility of the SPS process, which affords ample advantages for sizing-up and mass production of parts. Generally, when SPS is used to produce larger samples using the traditional approach of sintering without tooling assembly modifications, the samples exhibit variation in the temperature distribution which reduces as the Joule heat passing through the center of the sample dissipates from the core to the edges as shown in Fig. 17a. A similar limitation is observed with HIP when used to produce a larger sample, where the samples exhibit a temperature gradient decreasing from the edge to the core as shown in Fig. 17b, because of the sample being generally heated externally by heating coils.

To circumvent the limitations presented by the traditional HIP and SPS, an innovative type of SPS that incorporates an additional heating mode through induction heating by coils was developed. Through this blend of heating modes (Joule heating + induction heating) as illustrated in Fig. 18a, it is possible to produce larger specimens having good structural integrity due to unified heat distribution[124,127,128] as exemplified in Fig. 18b. The ability to produce disc specimens that are larger and yet achieve homogeneous heat distribution means that Hybrid-SPS has an advantage over traditional sintering processes as industrial products are rarely small. Several research works have been

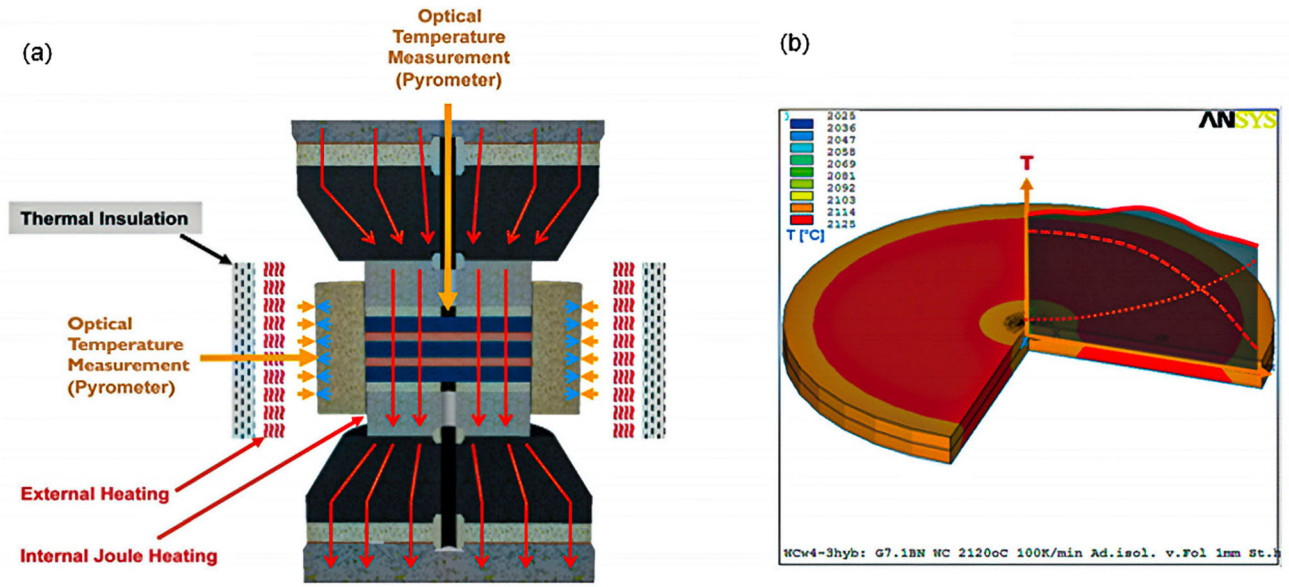

Fig. 18. (a) Principle of hybrid-SPS, the combination of classical hot pressing using an external heater, and internal Joule heating of SPS, (b) thermal gradients in a large disk sintered using Hybrid-SPS. Reprinted from Ref. 130, under the terms of the Creative Commons CC BY license.

successfully conducted for various materials using the hybrid-SPS.

The effectiveness of the sintering process is generally improved by using predictive simulation methods. Techniques such as numeric modeling assist with the prediction of sample sintering conditions, mold designs, and the prediction of properties of the obtained materials. Yushin et al.[131] modeled the process of SPS and hybrid-SPS of conducting (tungsten carbide) and non-conducting (aluminum oxide) powder materials by the finite element method. Their study showed that temperature variations in die molds and samples in SPS may be significant and the extent of variation depends also on the sample material's electric conductivity and sample and die dimensions, whereas hybrid heating comparatively improved the heat distribution and lowered the thermal gradients in the 80-mm-diameter samples of non-conducting material. This finding indicates the possibility of continuous mass production using hybrid-SPS on the industrial scale.

Grashchenkov et al.[132] sintered 100 mm HfB_2-based refractory ceramic material using a hybrid-SPS. The authors successfully obtained samples with the required quality using hybrid-SPS and not so when then they used the SPS. This was achieved by the combined heating mode of hybrid-SPS, which made it possible to obtain the necessary sintering temperature of 1800°C for the high melting point ceramic material. Conversely, they observed that the use of SPS heating mode alone resulted in a strong temperature gradient of about 150°C between the central part and the edge of the sample. The inhomogeneous thermal distribution can be accounted to the pathway of the Joule heating in SPS, which is generally from the core to the edges, which causes the heat dissipation to lessen as it moves from the core to the edges, especially with non-conducting materials.

Shongwe et al.[124] conducted a comparative study of SPS and hybrid-SPS of 93W-4.9Ni-2.1Fe alloy on 30 mm and 60 mm samples under similar environments. On completion of the SPS and hybrid-SPS processes, they discovered that both the 30 mm and 60 mm alloys had a relative density > 99.2%, except for the 60 mm sample sintered via SPS. The microstructure and mechanical properties of the 60 mm-SPS sample also showed a variation of properties from the edge to the core of the sample. Their work showed the effectiveness of hybrid-SPS in producing larger samples with good densification and homogeneous properties.

Hybrid-SPS has also been shown to be a beneficial process in obtaining complex-shaped samples, therefore, eliminating the need for cutting and machining processes. Kuznetsova et al.[133] successfully produced near-net-shaped Al2O3-SiCw ceramic nanocomposites through hybrid-SPS. The microstructure, mechanical, and wear properties of the samples were comparable to the sample cut-out from the standard SPS-sintered disk. Their study shows the great capabilities of the hybrid-SPS to fabricate excellent quality components in an economical way, an aspect that is advantageous to industries.

Large samples also mean that companies can reduce costs through the implementation of integrated technology that uses large manufactured structures thus reducing the number of components and joints.[134] With these numerous advantages, the hybrid-SPS technology represents a significant

opportunity to make a breakthrough in the industry as an innovative manufacturing process that has great potential to achieve productivity improvement. Specimens as large as 250 mm in diameter with a height of 16 mm[135] were successfully produced through this technology. Recently, a trial on a ceramic material was successful after a relative density of about 99% was obtained for a minimum holding time of 3 min, although high temperature and high pressure constituted this success.

The said observation of reported works on Hybrid-SPS serves as a great indication of postulated success in sintering larger TiAl specimens. Considering that TiAl is an electrically conductive material, samples with excellent densification and properties (microstructural, mechanical, and wear) can be accomplished even at relatively low sintering temperature and pressure. Furthermore, Hybrid SPS is a promising technology for the efficient manufacturing of large sizes of TiAl artifacts with homogeneous and fine grain size microstructure as a result of fast heating rate, low dwell temperature, and thermal gradient immanent to this special sintering technology. This is realized by the independent control of both the induction and Joule heating with temperature sensors attached to them thus providing a set-up that offsets possible radial thermal losses.

SUMMARY

Cost-effective titanium and alloy parts have been produced using a variety of powder metallurgy sintering technologies, such as cold pressing, and hot pressing. These manufacturing processes are limited in terms of the restrictions in control of the microstructural properties and phase evolution which inevitably affect the quality of the TiAl products. Due to the strong dependence of properties on the microstructure, an extensive range of properties can be reached by properly controlled heat treatment. The ability to control the process parameters will allow control of the basic microstructure, phase morphology, and precipitation reactions of titanium aluminide PM compacts and minimize porosity as all these factors are an integral part to optimize mechanical properties; see supplementary Table S-I for limitations and advantages of various PM methods for fabrication of TiAl alloys and supplementary Table S-II for the summary of various PM methods for fabrication of TiAl alloys and the obtained relative densities, hardness and phase compositions (refer to online supplementary material). Whether the new materials can be manufactured and tested at reasonable costs will ultimately influence their rate of introduction in commercial aircraft and automobiles, whereas rapid synthesis methods are proven to be cost-effective and easy to use but produces highly porous structures and required additional densification steps to increase relative densities. On the other hand, the concept of spark plasma sintering could prove to offer a step change in the manufacturing of titanium aluminide components by providing flexible control of the process and thus providing a breakthrough into commercial applications of powder metallurgy products. The recent development of combination heating of Joule heating and induction heating presents the possibilities of mass production of simple disk shape TiAl samples in one die, indicating that with proper mold designs and empirical models, mass production of complex shape components can be achieved. Further investigation of the SPS and hybrid-SPS process for producing TiAl is required for improved accuracy and quality of the material, which can be achieved using predictive numerical models and empirical tests. Thus, the data (see supplementary Table S-III for a summary of available literature on hybrid-SPS, refer to online supplementary material) may be utilized for the advancement in the processing of innovative materials using SPS and hybrid-SPS depending on the material, size, and shape.

ACKNOWLEDGEMENTS

This research is supported by National Research Foundation (NRF) under the New Generation of Academics Programme (nGAP).

CONFLICT OF INTEREST

On behalf of all authors, the corresponding author states that there is no conflict of interest.

REFERENCES

1. H. Clemens and H. Kestler, *Adv. Eng. Mater.* 2(9), 551 (2000).
2. P.A. Bartolotta and D.L. Krause, Titanium aluminide applications in the high speed civil transport (No. NASA/TM-1999-209071).
3. B.P. Bewlay, S. Nag, A. Suzuki, and M.J. Weimer, *Mater. High Temp.* 33(4–5), 549 (2016).
4. B. Liu, Y. Liu, C. Qiu, C. Zhou, J. Li, H. Li, and Y. He, *J. Alloy. Compd.* 640, 298 (2015).
5. A. Couret, G. Molénat, J. Galy, and M. Thomas, *Intermetallics* 16(9), 1134 (2008).
6. A. Pineau, A.A. Benzerga, and T. Pardoen, *Acta Mater.* 107, 508 (2016).
7. S. Yang and W. Li, Surface quality and finishing technology, *Surface Finishing Theory and New Technology* (Springer, Berlin, 2018), pp. 1–64.
8. H. Huang, H. Ding, and X. Xu, *Procedia Manuf.* 37, 73 (2019).
9. A. Duarte, F. Viana, and H.M. Santos, *Mater. Res.* 2, 191 (1999).
10. V. Küstner, M. Oehring, A. Chatterjee, *Gamma Titanium Aluminides*, vol. 2003 (2003), p. 89.
11. R. Gerling, H. Clemens, and F. Schimansky, *Adv. Eng. Mater.* 6(1–2), 23 (2004).
12. P. Ramakrishnan, Automotive applications of powder metallurgy, *Advances in Powder Metallurgy*, ed. I. Chang and Y. Zhao (Elsevier, Amsterdam, 2013), p. 493.
13. T. Voisin, L. Durand, N. Karnatak, S. Le Gallet, M. Thomas, Y. Le Berre, J.F. Castagné, and A. Couret, *J. Mater. Process. Technol.* 213(2), 269 (2013).
14. Z. Trzaska, A. Couret, and J.-P. Monchoux, *Acta Mater.* 118, 100 (2016).

15. D. Martins, F. Grumbach, A. Simoulin, P. Sallot, K. Mocellin, M. Bellet, and C. Estournès, *Mater. Sci. Eng. A* 711, 313 (2018).
16. K. Kothari, R. Radhakrishnan, and N.M. Wereley, *Prog. Aerosp. Sci.* 55, 1 (2012).
17. F. Appel, J.D.H. Paul, and M. Oehring, *Gamma Titanium Aluminide Alloys* (Wiley, New Jersey, 2011).
18. F.H. Froes, S.J. Mashl, J.C. Hebeisen, V.S. Moxson, and V.A. Duz, *JOM* 56(11), 46 (2004).
19. M. Qian, *Int. J. Powder Metall.* 46(5), 29 (2010).
20. W.X. Yuan, J.F. Mei, V. Samarov, D. Seliverstov, and X.H. Wu, *J. Mater. Process. Technol.* 182(1–3), 39 (2007).
21. H. Yu, C. Lu, A.K. Tieu, H. Li, A. Godbole, and C. Kong, *Mater. Sci. Eng. A* 660, 195 (2016).
22. L. Chen, J. Lin, X. Xu, C. Li, Y. Xu, and Y. Liang, *J. Alloys Compd.* 741, 1175 (2018).
23. G. Molénat, A. Couret, M. Thomas, and J. Galy, *Sintering 1-intermetallics & high temperature materials: processing of TiAl alloys by spark plasma sintering*, in *European Congress and Exhibition on Powder Metallurgy. European PM Conference Proceedings*. The European Powder Metallurgy Association, vol 3, no. 2, p. 83 (2007).
24. G. Lee, E.A. Olevsky, C. Manière, A. Maximenko, O. Izhvanov, C. Back, and J. McKittrick, *Acta Mater.* 144, 524 (2018).
25. O. Guillon, J. Gonzalez-Julian, B. Dargatz, T. Kessel, G. Schierning, J. Räthel, and M. Herrmann, *Adv. Eng. Mater.* 16(7), 830 (2014).
26. E.A. Olevsky and L. Froyen, *J. Am. Ceram. Soc.* 92, 122 (2009).
27. H. Clemens and S. Mayer, *Mater. High Temp.* 33(4–5), 560 (2016).
28. T. Klein, H. Clemens, and S. Mayer, *Materials* 9(9), 755 (2016).
29. V.V. Kurbatkina, Titanium aluminides, in *Concise Encyclopedia of Self-Propagating High-Temperature Synthesis*. ed. by I.P. Borovinskaya, A.A. Gromov, E.A. Levashov, Y.M. Maksimov, A.S. Mukasyan, and A.S. Rogachev (Elsevier, New York, 2017), p. 392.
30. S. Djanarthany, J.-C. Viala, and J. Bouix, *Mater. Chem. Phys.* 72(3), 01 (2001).
31. J. Fan, X. Li, Y. Su, J. Guo, and H. Fu, *Mater. Des.* 34, 552 (2012).
32. V. Güther, C. Rothe, S. Winter, and H. Clemens, *BHM Berg-und Hüttenmännische Monatshefte* 155(7), 325 (2010).
33. H. Clemens and S. Mayer, *Trans. Tech. Publ.* 879, 113 (2017).
34. H.-W. Liu and K.P. Plucknett, *Adv. Powder Technol.* 28(1), 314 (2017).
35. R.M. Imayev, V.M. Imayev, M. Oehring, and F. Appel, *Intermetallics* 15(4), 451 (2007).
36. P.V. Cobbinah and W.R. Matizamhuka, *Adv. Mater. Sci. Eng.* 2, 1 (2019).
37. S.A. Jones, R.D. Shull, A.J. McAlister, and M.J. Kaufman, *Scr. Metall.* 22(8), 1235 (1988).
38. D. Wimler, J. Lindemann, T. Kremmer, H. Clemens, and S. Mayer, *Intermetallics* 138, 107316 (2021).
39. M. Oehring, F. Appel, T. Pfullmann, and R. Bormann, *Appl. Phys. Lett.* 66(8), 941 (1995).
40. J.R. Kennedy, D. Daloz, B. Rouat, E. Bouzy, and J. Zollinger, *Intermetallics* 95, 89 (2018).
41. B. Liu, M. Wang, Y. Du, and J. Li, *Materials* 13(1), 161 (2020).
42. B. Duan, Y. Yang, S. He, Q. Feng, L. Mao, X. Zhang, L. Jiao, X. Lu, G. Chen, and C. Li, *J. Alloys Compd.* 909, 164811 (2022).
43. J.P. Immarigeon, R.T. Holt, A.K. Koul, L. Zhao, W. Wallace, and J.C. Beddoes, *Mater. Charact.* 35(1), 41 (1995).
44. P. Novák, P. Salvetr, and Z. Pecenová, *Manuf. Technol.* 15(6), 1024 (2015).
45. M. Gebler, A.J.S. Uiterkamp, and C. Visser, A global sustainability perspective on 3D printing technologies. *Energy Policy* 74, 158 (2014).
46. E. Baumeister and S. Klaeger, *Adv. Eng. Mater.* 5(9), 673 (2003).
47. I. Robertson and G. Schaffer, *Powder Metall.* 53(2), 146 (2010).
48. S. Sovizi and M.E. Seraji, *Sci. Sinter.* 51(2), 135 (2019).
49. T.M. Motsai, S. Chikosha, C. Machio, and M.E. Makhatha, A comparative study of oxygen pick-up of TiHDH powder during press and sinter and loose sintering processing. in *IOP Conference Series: Materials Science and Engineering*, IOP Publishing, vol. 430, no. 1, p. 012031 (2018).
50. A. Govender, C. Bemont, and S. Chikosha, *Metals* 11(6), 936 (2021).
51. J. Alves Nogueira da Silva, L. Quaglio, W. Alves Monfardini, and J. Soyama, *Mater. Sci. Technol.* 39, 1 (2022).
52. A.L. Rominiyi, M.B. Shongwe, L.C. Tshabalala, E.N. Ogunmuyiwa, S.O. Jeje, B.J. Babalola, and P.A. Olubambi, *J. Alloys Compd.* 848, 156559 (2020).
53. A. Krairi, K. Matouš, and A. Salvadori, *Int. J. Solids Struct.* 135, 89 (2018).
54. U.M. Attia, *Crit. Rev. Solid State Mater. Sci.* 46(6), 587 (2021).
55. C. Turner and M. Ashby, *Acta Mater.* 44(11), 4521 (1996).
56. M. Yan, F. Yang, B. Lu, C. Chen, Y. Sui, and Z. Guo, *Metals* 11(4), 635 (2021).
57. Y. Xia, G.B. Schaffer, and M. Qian, *Trans. Tech. Publ.* 520, 89 (2012).
58. E. Fu, R. Rawlings, and H. McShane, *J. Mater. Sci.* 36(23), 5537 (2001).
59. E. Calvert, B. Wynne, N. Weston, A. Tudball, and M. Jackson, *J. Mater. Process. Technol.* 254, 158 (2018).
60. N. Gupta and B. Basu, Hot pressing and spark plasma sintering techniques of intermetallic matrix composites, *Intermetallic Matrix Composites*, ed. R. Mitra (Elsevier, New York, 2018), pp. 243–302.
61. N. Reddy, H.J. Choi, and H.B. Young, *Korean J. Mater. Res.* 24(7), 381 (2014).
62. Y.F. Yang and M. Qian, Spark plasma sintering and hot pressing of titanium and titanium alloys, *Titanium Powder Metallurgy*, ed. M.A. Qian and F.H. Froes (Elsevier, New York, 2015), pp. 219–235.
63. A.V. Muley, S. Aravindan, and I. Singh, *Manuf. Rev.* 2, 15 (2015).
64. U. Habel and B.J. McTiernan, *Intermetallics* 12(1), 63 (2004).
65. B.W. Choi, Y.G. Deng, C. McCullough, B. Paden, and R. Mehrabian, *Acta Metall. Mater.* 38(11), 2225 (1990).
66. S. Semiatin, G. Cornish, and D. Eylon, *Mater. Sci. Eng. A* 185(1–2), 45 (1994).
67. V. Samarov, C. Barre, D. Seliverstov, E. Khomyakov, and R. Haykin, *Net shape HIP for complex shape PM parts as a cost-efficient industrial technology*, in *Proceedings of 2005 International Conference on Hot Isostatic, Pressing, Paris*, vol. 48 (2005).
68. K. Naplocha, Self-propagating high-temperature synthesis (SHS) of intermetallic matrix composites, *Intermetallic Matrix Composites*, ed. R. Mitra (Elsevier, New York, 2018), pp. 203–220.
69. M. Adeli, S.H. Seyedein, M.R. Aboutalebi, M. Kobashi, N. Kanetake, *The self-propagating high temperature synthesis of titanium aluminides: a parametric study*. in *Proceedings of the 2nd World Congress on Mechanical, Chemical, and Material Engineering (MCM'16), Budapest, Hungary* (2016).
70. W. Garrett, *Control of Self-Propagating High-Temperature Synthesis Derived Aluminum-Titanium Carbide Metal Matrix Composites*, (Colorado School of Mines ProQuest Dissertations Publishing, United States (2013).
71. C. Farley, T. Turnball, M.L. Pantoya, and E.M. Hunt, *Acta Mater.* 59(6), 2447 (2011).
72. H. Agripa and I. Botef, Modern production methods for titanium alloys: a review, in *Titanium Alloys-Novel Aspects of Their Manufacturing and Processing*. ed. by M. Motyka, W. Ziaja, and J. Sieniawski (BoD Books on Demand, Philippines, 2019).

73. M. Adeli, S.H. Seyedein, M.R. Aboutalebi, M. Kobashi, and N. Kanetake, *J. Alloys Compd.* 497(1–2), 100 (2010).
74. E.M. Hunt, K.B. Plantier, and M.L. Pantoya, *Acta Mater.* 52(11), 3183 (2004).
75. B.Y. Li, L.J. Rong, Y.Y. Li, and V.E. Gjunter, *Acta Mater.* 48(15), 3895 (2000).
76. V. Vershinnikov and I. Borovinskaya, *Powder Metall. Met. Ceram.* 48(9), 533 (2009).
77. M. Singh, S.O. Lara, and S. Tlali, *J. Taibah Univ. Sci.* 11(6), 922 (2017).
78. G. Guisbiers, M. Kazan, O. Van Overschelde, M. Wautelet, and S. Pereira, *J. Phys. Chem. C* 112(11), 4097 (2008).
79. X. Yu and Z. Zhan, *Nanoscale Res. Lett.* 9(1), 1 (2014).
80. M.A. Shandiz and A. Safaei, *Mater. Lett.* 62(24), 3954 (2008).
81. H. Sohn and X. Wang, *Mater. Manuf. Process* 9(1), 75 (1994).
82. E. Medda, F. Delogu, and G. Cao, *Mater. Sci. Eng. A* 361(1–2), 23 (2003).
83. R. Orru, G. Cao, and Z. Munir, *Metall. Mater. Trans. A.* 30(4), 1101 (1999).
84. L. Kecskes, B. Butler, G. Oniashvili, Z. Aslamazishvili, G. Zakharov, and A. Peikrishvili, *Mater. Manuf. Process.* 26(9), 1157 (2011).
85. X. Jiao, X. Cai, G. Niu, X. Ren, X. Kang, and P. Feng, *Prog. Nat. Sci. Mater. Int.* 29(4), 447 (2019).
86. M.A. Lagos, I. Agote, M. Gutiérrez, A. Sargsyan, and L. Pambaguian, *Int. J. Self Propag. High Temp. Synth.* 19(1), 23 (2010).
87. A. Borrell and M.D. Salvador, Advanced ceramic materials sintered by microwave technology, in *Sintering Technology: Method and Application*. ed. by M. Liu (BoD Books on Demand, Philippines, 2018), pp. 3–24.
88. R.D. Peelamedu, R. Roy, and D. Agrawal, *Mater. Res. Bull.* 36(15), 2723 (2001).
89. S. Raynova, M.A. Imam, F. Yang, and L. Bolzoni, *J. Manuf. Process.* 39, 52 (2019).
90. D.E. Clark and W.H. Sutton, *Annu. Rev. Mater. Sci.* 26(1), 299 (1996).
91. J. Sun, W. Wang, and Q. Yue, *Materials* 9(4), 231 (2016).
92. R. Roy, D. Agrawal, J. Cheng, and S. Gedevanishvili, *Nature* 399(6737), 668 (1999).
93. E. Yoshikawa, E. Ishizuka, and S. Taniguchi, *Mater. Trans.* 47(3), 898 (2006).
94. S.D. Luo, C.L. Guan, Y.F. Yang, G.B. Schaffer, and M. Qian, *Metall. Mater. Trans. A.* 44(4), 1842 (2013).
95. V.D. Buchelnikov, D.V. Louzguine-Luzgin, G. Xie, S. Li, N. Yoshikawa, M. Sato, A.P. Anzulevich, I.V. Bychkov, and A. Inoue, *J. Appl. Phys.* 104(11), 113505 (2008).
96. J. Vleugels, I. Volders, S. Put, C. Zhao, O. Van der Biest, C. Groffils, P.J. Luypaert, G. Barbier, L. Bourgeois, Hybrid-microwave sintering of hardmetals and graded oxides composites, in *Proceedings in International Plansee Seminar, Reutte*, *Austria* (2001).
97. C. Singhal and Q. Murtaza, Microwave sintering of advanced composites materials: a review. *Mater. Today Proc.* 5(11), 24287 (2018).
98. S. Jayalakshmi, R.A. Singh, and M. Gupta, *Technologies* 6(2), 40 (2018).
99. A.S. Awad, D. Merheb, M. Zakhour, M. Nakhl, and J.L. Bobet, *J. Alloys Compd.* 720, 182 (2017).
100. W. Chen, J. Tang, X. Lin, Y. Ai, and N. Ye, *Materials* 13(23), 5356 (2020).
101. S.D. Luo, Y.F. Yang, G.B. Schaffer, and M. Qian, *Scripta Mater.* 69(1), 69 (2013).
102. C. Arnaud, C. Manière, G. Chevallier, C. Estournès, R. Mainguy, F. Lecouturier, D. Mesguich, A. Weibel, L. Durand, and C. Laurent, *J. Mater. Sci.* 50(22), 7364 (2015).
103. C. Manière, E. Nigito, L. Durand, A. Weibel, Y. Beynet, and C. Estournès, Spark plasma sintering and complex shapes: the deformed interfaces approach. *Powder Technol.* 320, 340 (2017).
104. E.L. Calvert, A.J. Knowles, J.J. Pope, D. Dye, and M. Jackson, *Scripta Mater.* 159, 51 (2019).
105. E. Khaleghi, Y.S. Lin, M.A. Meyers, and E.A. Olevsky, *Scripta Mater.* 63(6), 577 (2010).
106. M.R. Mphahlele, E.A. Olevsky, and P.A. Olubambi, Spark plasma sintering of near net shape titanium aluminide: a review, in *Spark Plasma Sintering*. ed. by G. Cao, C. Estournès, J. Garay, and R. Orrù (Elsevier, New York, 2019), pp. 281–299.
107. E. Olevsky and D. Dudina, *Field-Assisted Sintering. Science and Applications* (Springer, New York, 2018).
108. K. Matsugi, N. Ishibashi, T. Hatayama, and O. Yanagisawa, *Intermetallics* 4(6), 457 (1996).
109. D. Wang, H. Yuan, and J. Qiang, *Metals* 7(6), 201 (2017).
110. B.-N. Kim, K. Hiraga, K. Morita, and H. Yoshida, *J. Eur. Ceram. Soc.* 29(2), 323 (2009).
111. A.A. ldoshan, *Spark Plasma Sintering of Titanium Aluminide Intermetallics and Its Composites* (Oklahoma State University, Stillwater, 2012).
112. Y.-W. Kim and D.M. Dimiduk, *JOM* 43(8), 40 (1991).
113. G. Molénat, M. Thomas, J. Galy, and A. Couret, *Adv. Eng. Mater.* 9(8), 667 (2007).
114. S.-L. Xiao, T.I.A.N. Jing, L.J. Xu, Y.Y. Chen, H.B. Yu, and J.C. Han, *Trans. Nonferrous Met. Soc. China* 19(6), 1423 (2009).
115. J. Wang, Y. Wang, Y. Liu, J. Li, L. He, and C. Zhang, *Intermetallics* 64, 70 (2015).
116. M. Bambach, A. Emdadi, I. Sizova, U. Hecht, and F. Pyczak, *Intermetallics* 101, 44 (2018).
117. X. Li, H. Xu, W. Xing, B. Chen, Y. Ma, and K. Liu, *Metals* 8(9), 731 (2018).
118. Y. Xia, J. Zhao, and M. Qian, *JOM* 71(8), 2556 (2019).
119. D. Giuntini, E.A. Olevsky, C. Garcia-Cardona, A.L. Maximenko, M.S. Yurlova, C.D. Haines, D.G. Martin, and D. Kapoor, *Materials* 6(7), 612 (2013).
120. X. Gu, F. Cao, N. Liu, G. Zhang, D. Yang, H. Shen, D. Zhang, H. Song, and J. Sun, *J. Alloys Compd.* 819, 153264 (2020).
121. H. He, L. Zhang, S. Li, X. Wu, H. Zhang, and L. Li, *Metals* 8(1), 39 (2018).
122. M.S. El-Eskandarany, *Mechanical Alloying: Nanotechnology, Materials Science and Powder Metallurgy* (Elsevier, New York, 2015).
123. N. Weston and M. Jackson, *J. Mater. Process. Technol.* 243, 335 (2017).
124. M.B. Shongwe, S. Diouf, M.O. Durowoju, P.A. Olubambi, M.M. Ramakokovhu, and B.A. Obadele, *Int. J. Refract. Met. Hard Mater.* 55, 16 (2016).
125. C. Manière, L. Durand, A. Weibel, G. Chevallier, and C.A. Estournès, *Scripta Mater.* 124, 126 (2016).
126. T. Voisin, J.P. Monchoux, L. Durand, N. Karnatak, M. Thomas, and A. Couret, *Adv. Eng. Mater.* 17(10), 1408 (2015).
127. J.R. Groza and A. Zavaliangos, *Mater. Sci. Eng. A* 287(2), 171 (2000).
128. M. Suárez, A. Fernández, J.L. Menéndez, R. Torrecillas, H.U. Kessel, J. Hennicke, R. Kirchner, and T. Kessel, *Sinter. Appl.* 13, 319 (2013).
129. J. Hennicke, T. Kessel, and J. Raethel, Enhancements on fast sintering systems promote transfer from the lab to industrial applications, *Advanced Processing and Manufacturing Technologies for Nanostructured and Multifunctional Materials III*, ed. T. Ohji, M. Singh, M. Halbig, and K. Moon, Vol. 11 (The American Ceramic Society, Daytona Beach, FL, USA, 2017), pp, 11–20.
130. J. Hennicke, T. Kessel, and S.R. Monte, *Hybrid Sintering—A New Trend for Innovative Material Solutions*, vol. 95, no. 8 (2018).
131. D.I. Yushin, A.V. Smirnov, N.W. Solis Pinargote, P.Y. Peretyagin, and R. Torrecillas San Millan, *Modeling process of spark plasma sintering of powder materials by finite element method*. in *Materials Science Forum*, vol. 834 (Trans Tech Publ., 2015), p. 41.
132. D.V. Grashchenkov, O.Y. Sorokin, Y.E. Lebedeva, and M.L. Vaganova, *Russ. J. Appl. Chem.* 88(3), 386 (2015).

133. E. Kuznetsova, P. Peretyagin, A. Smirnov, W. Solis, and R. Torrecillas, *Near-net shapes Al_2O_3-SiC w ceramic nanocomposites produced by hybrid spark plasma sintering*, in *Proceedings of the Scientific-Practical Conference "Research and Development-2016"* (2018), p. 397.
134. A. Heinz, A. Haszler, C. Keidel, S. Moldenhauer, R. Benedictus, and W.S. Miller, *Mater. Sci. Eng. A* 280(1), 102 (2000).
135. F. Vogeler, A. Migdal, B. Lauwers, and E. Ferraris, The effect of wire-edm processing on the flexural strength of large scale ZrO2-TiN. *Proc. CIRP* 45, 179 (2016).